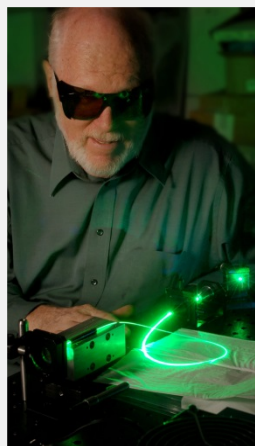
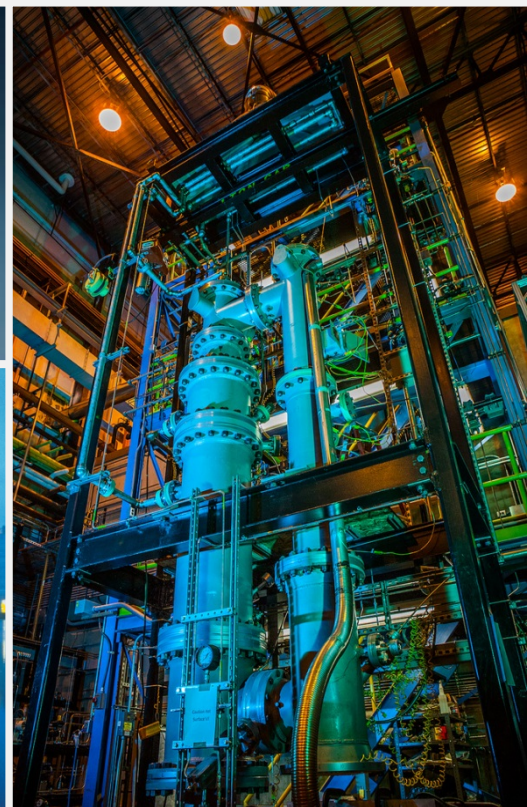
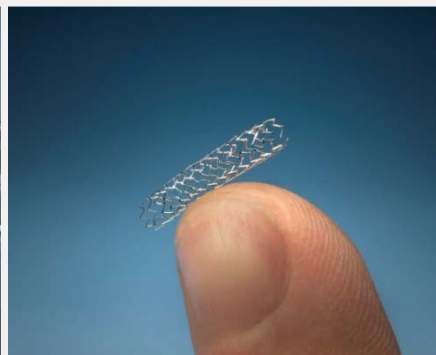
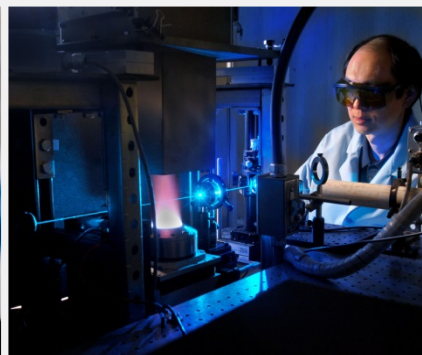




Driving Innovation ♦ Delivering Results



High-Temperature Corrosion of Diffusion Bonded Ni-Based Superalloys in CO₂

Ömer Doğan
Casey Carney
Richard Oleksak
Corinne Disenhof
Gordon Holcomb



Acknowledgements



Monica Kapoor
Joe Tylczak
Trevor Godell



Aaron Wilson
Thomas L'Estrange
Kevin Drost



Vinod Narayanan

This project is conducted in support of DOE-FE Advanced Combustion Program (Richard Dennis and Daniel Driscoll, Technology Managers and Briggs White, Project Monitor) and is executed through NETL Research and Innovation Center's Advanced Combustion Field Work Proposal.

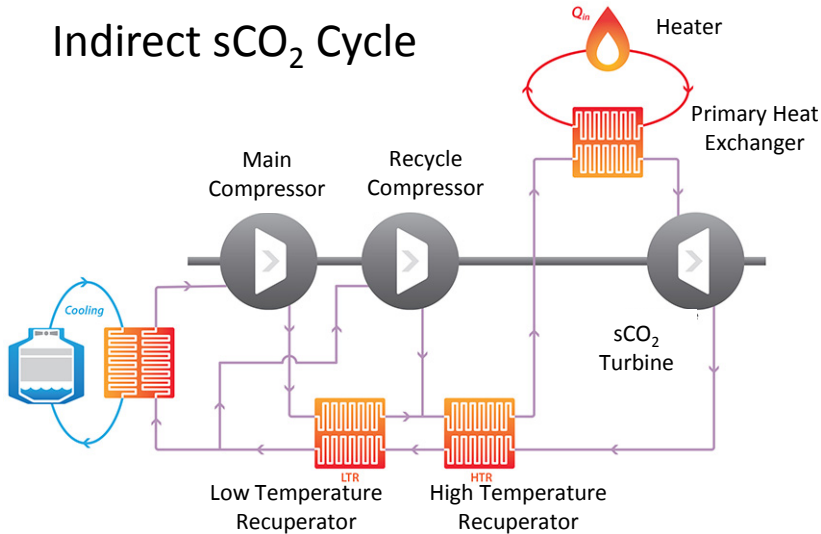
DISCLAIMER

"This report was prepared as an account of work sponsored by an agency of the United States Government. Neither the United States Government nor any agency thereof, nor any of their employees, makes any warranty, express or implied, or assumes any legal liability or responsibility for the accuracy, completeness, or usefulness of any information, apparatus, product, or process disclosed, or represents that its use would not infringe privately owned rights. Reference herein to any specific commercial product, process, or service by trade name, trademark, manufacturer, or otherwise does not necessarily constitute or imply its endorsement, recommendation, or favoring by the United States Government or any agency thereof. The views and opinions of authors expressed herein do not necessarily state or reflect those of the United States Government or any agency thereof."

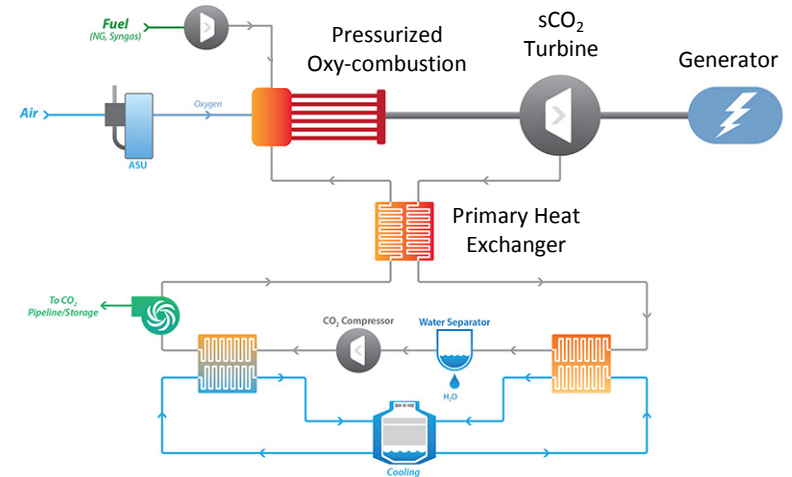
Supercritical CO₂ Power Cycles



Indirect sCO₂ Cycle



Direct sCO₂ Cycle



Cycle/Component		Inlet		Outlet	
		T (C)	P (MPa)	T (C)	P (MPa)
Indirect	Heater	450-535	1-10	650-750	1-10
	Turbine	650-750	20-30	550-650	8-10
	HX	550-650	8-10	100-200	8-10
Direct	Combustor	750	20-30	1150	20-30
	Turbine	1150	20-30	800	3-8
	HX	800	3-8	100	3-8

Essentially pure CO₂

CO₂ with combustion products including H₂O, O₂, and SO₂

Compact Heat Exchangers



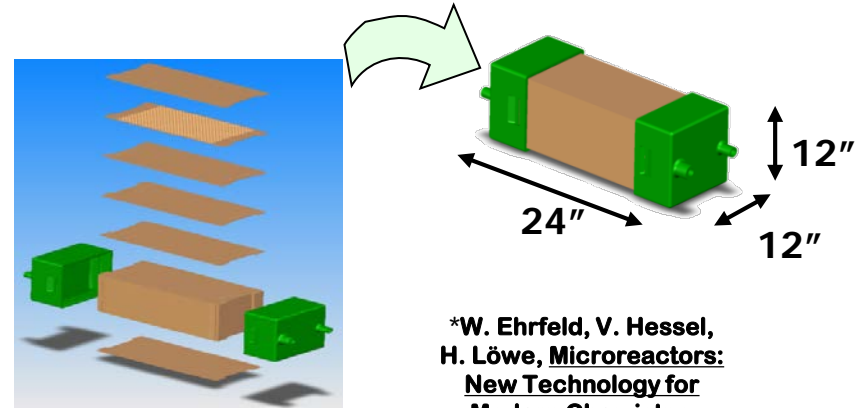
- **Higher efficiency**
 - Due to much shorter heat diffusion lengths in fluid
- **Smaller size**
 - Use of less materials (expensive superalloys)
 - Takes less space
- **Modular design**
 - Expandable to large power plants

Typical Microchannel HX Fabrication Process

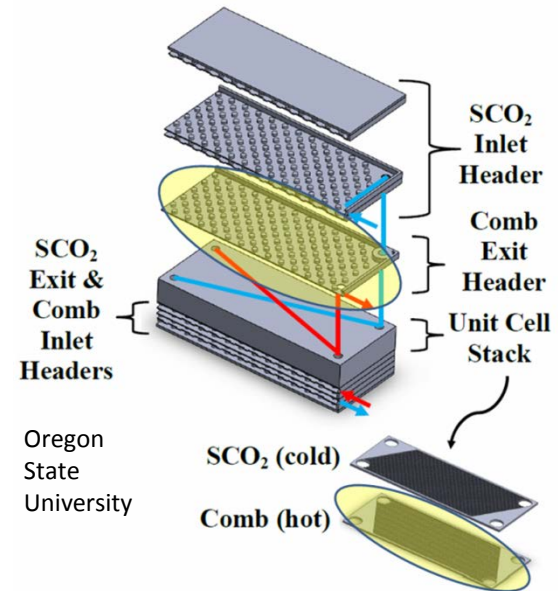


Microlamination-

1. Pattern microscale flow paths into laminae using a variety of methods (etching, micromachining, laser cutting, EDM, others)
2. Bond these laminae using a variety of methods (diffusion bonding, laser welding, brazing, others). For $s\text{CO}_2$, diffusion bonding and brazing are the most robust approaches



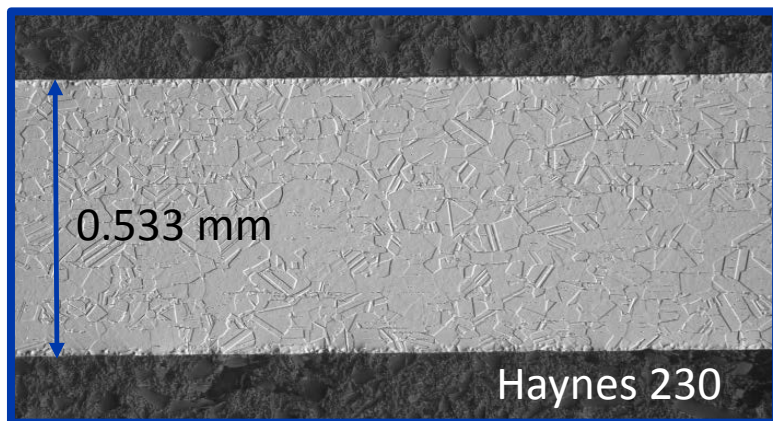
*W. Ehrfeld, V. Hessel, H. Löwe, Microreactors: New Technology for Modern Chemistry, Wiley-VCH, 2000.



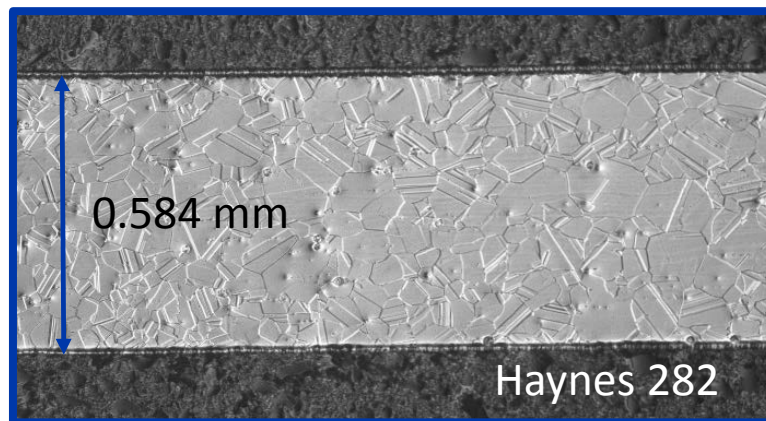
Nominal chemical composition (weight %) of materials used in this study
(Haynes 230 and Haynes 282)

	Ni	Cr	W	Ti	Mo	Fe	Co	Mn	Si	Al	C	B
H230	57	22	14	--	2	3*	5*	0.5	0.4	0.3	0.10	0.015*
H282	57	19.5	--	2.1	8.5	1.5*	10	0.3*	0.15*	1.5	0.06	0.005

* = maximum



Solid-solution strengthened
Cold rolled and 1232 °C solution annealed sheet

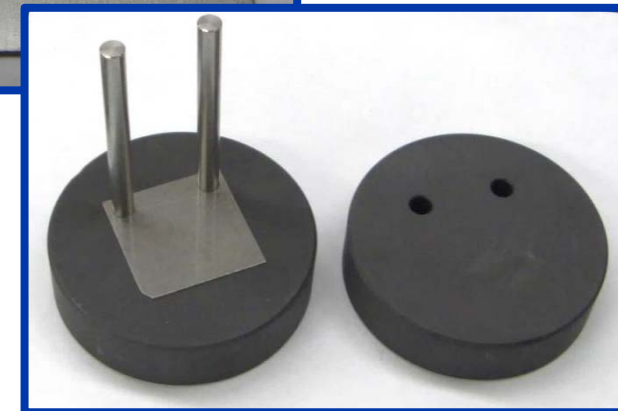
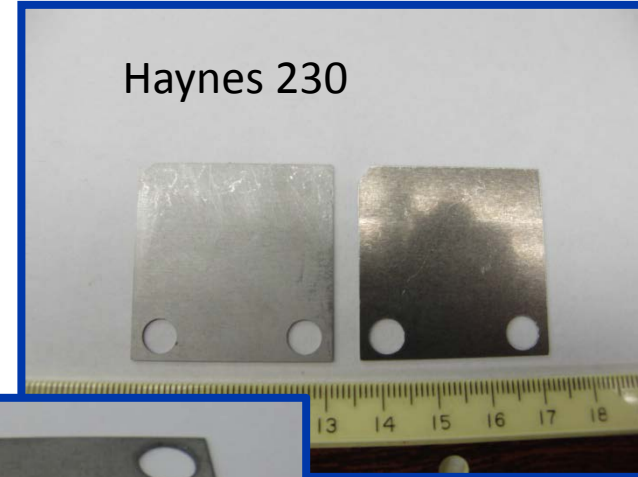


Precipitation strengthened
1149 °C solution annealed sheet

Diffusion Bonding



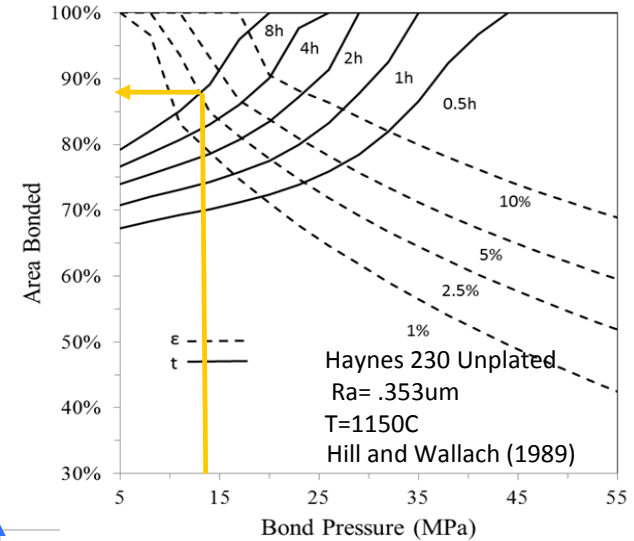
- Sheets were water-jet cut into shims
- 100 shims were bonded together in each stack
- All shims were reverse current etched and cleaned with acetone
- Some stacks used shims plated with electroless nickel, 2 - 4 μm thick
- Some shims contained pin-fin microfeatures identical to those used in a heat exchanger
- All shims were thoroughly cleaned by hand and in an ultrasonic acetone bath for 15 minutes immediately before bonding



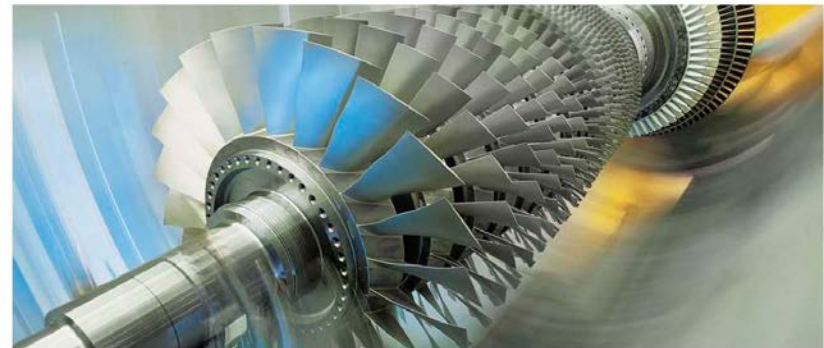
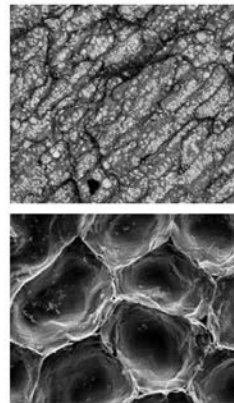
Diffusion Bonding



- Shim stacks were held in a fixture during bonding and pressure was applied only after the temperature ramped up to the desired value
- The hot press vacuum was maintained at approximately 5×10^{-6} torr (0.0007 Pa)
- 1150°C for 8 hours at 12.7 MPa
- After bonding, each stack was machined to produce 6 tensile specimens using wire EDM and a CNC lathe
- After bonding, H230 experienced approximately 4.1% strain (2.5% predicted by model)
- H282 without Ni plating did not bond well



Wednesday – March 30th
8:50 am
Session: Heat Exchangers III
Salon A



Diffusion Bonding of H230 Ni-superalloy for application in microchannel heat exchangers

*The 5th International Symposium - Supercritical CO₂ Power Cycles
March 28-31, 2016, San Antonio, Texas*

*M. Kapoor, Ö. Doğan, K. Rozman, J. Hawk,
A. Wilson, T. L'Estrange, V. Narayanan*

March 30th 2016

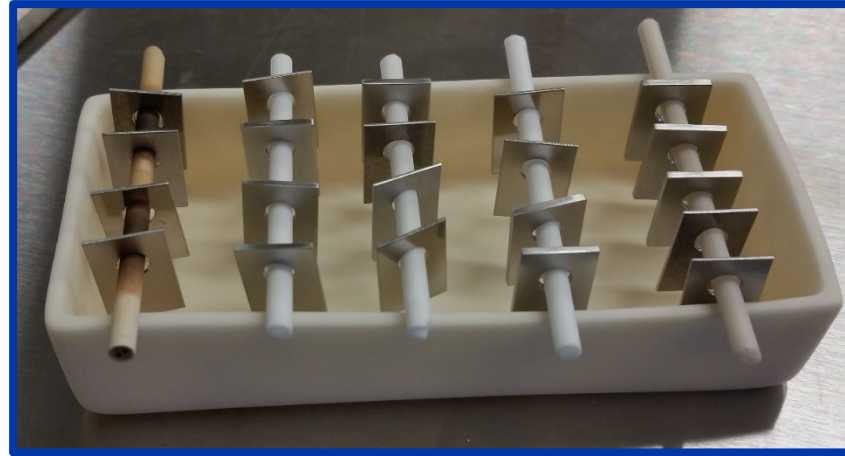
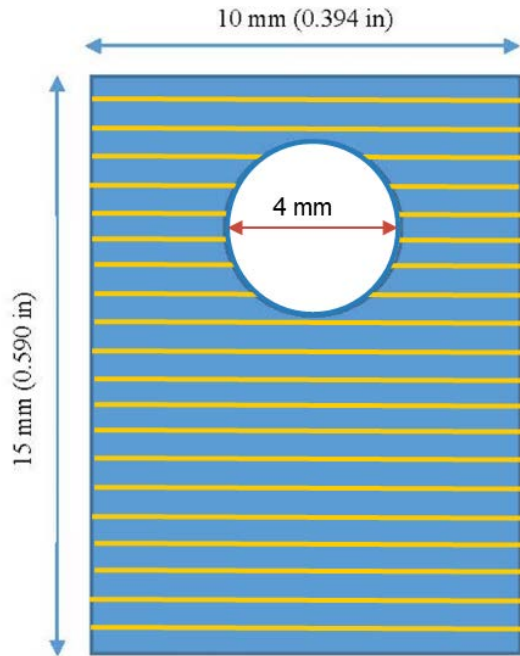
Diffusion Bonding



- **Diffusion bonding is the “weak link” in the fabrication process**
- **Sharp edges in the architecture lead to locations of high stress concentration in the mechanical design simulations**
- **We need information on**
 - The parameters for diffusion bonding (T, P, t) for these superalloys
 - The strength of the diffusion bond
 - Whether the high stress concentration predicted by the mechanical design simulations is indeed a problem or not.
 - Corrosion behavior of diffusion bonded regions in sCO₂



Oxidation tests



Characterization
Mass Change
XRD
SEM

Gas: 1 bar CO₂ (99.999% purity)
Gas flow rate: 0.032 kg/h
Temperature: 700°C
Duration: 500 h
24 h purging with CO₂ before heating



- Unlike in sH_2O , there is no evidence of increased oxidation rates at high pressure in sCO_2

Thursday – March 31st
 9:00 am
 Session: Materials I
 Salon C



NETL *Driving Innovation ♦ Delivering Results*

Materials Performance in Supercritical CO_2 in Comparison with Atmospheric CO_2 and Supercritical Steam

Gordon R Holcomb, Ömer N. Doğan, Casey Carney, Kyle Rozman, Jeffrey A. Hawk, and Mark Anderson

The 5th International Symposium - Supercritical CO_2 Power Cycles - March 28-31, 2016, San Antonio, TX

U.S. DEPARTMENT OF **ENERGY** National Energy Technology Laboratory

Oxidation Results



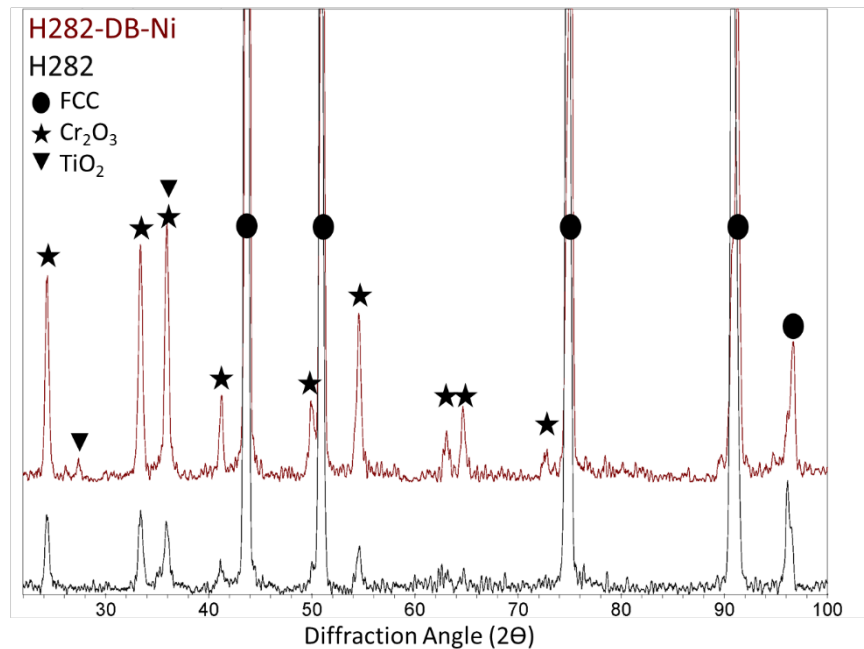
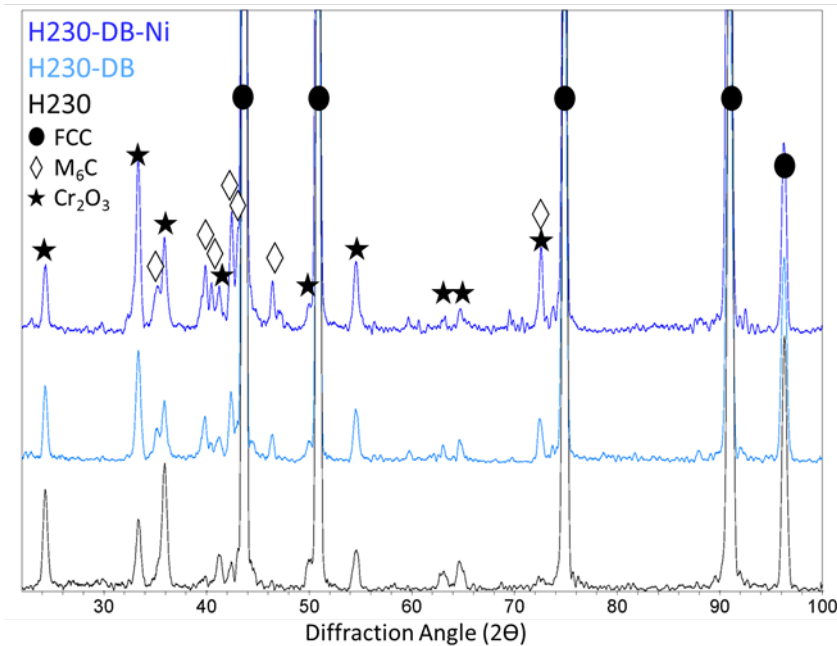
Mass changes as a result of the CO₂ exposure at 700°C for 500 h. Averages and standard deviations are from three coupons for each condition.

	Average mass change (mg/cm ²)	Standard deviation (mg/cm ²)
H230	0.077	0.012
H230-DB	0.115	0.013
H230-DB-Ni	0.112	0.005
H282	0.038	0.022
H282-DB-Ni	0.236	0.008

H230: Minor mass change increase

H282: More significant mass change increase

XRD on the Oxidized Samples



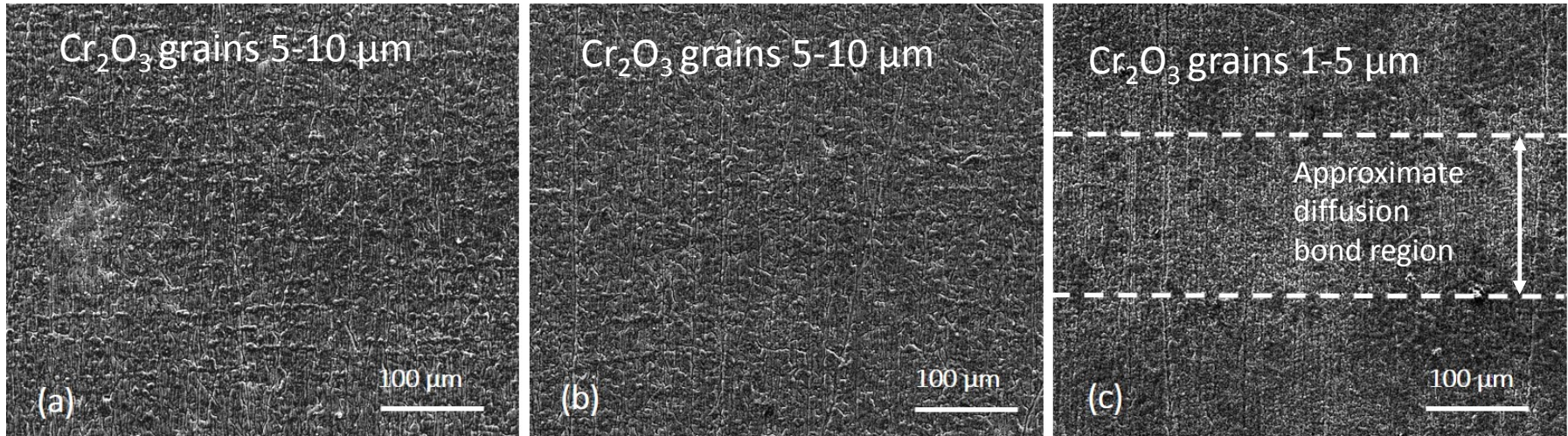
XRD signal from both oxide scale and underlying alloy

Chromia oxide scales form on both alloys

H230 contains W and Mo rich M_6C carbides

H282 contains γ' precipitates, $Ni_3(Al,Ti)$, but was not detected by XRD

SEM on the surface of oxidized samples



H230-DB-Ni

H230-DB

H282-DB-Ni

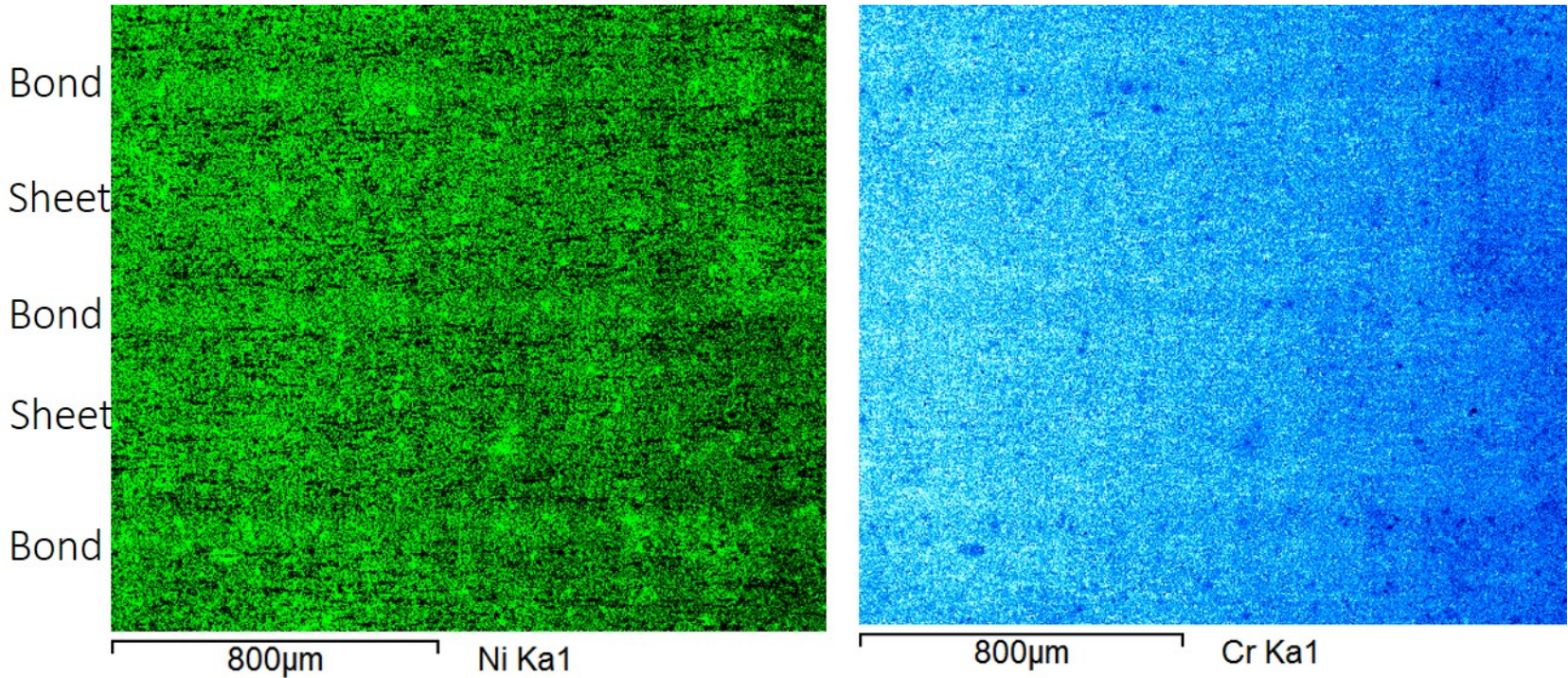
Dense, fine-grained, oxide scales

No observed differences in H230 between bond and non-bond areas

Some contrast differences in H282 in and near bond areas

Secondary Electron Images

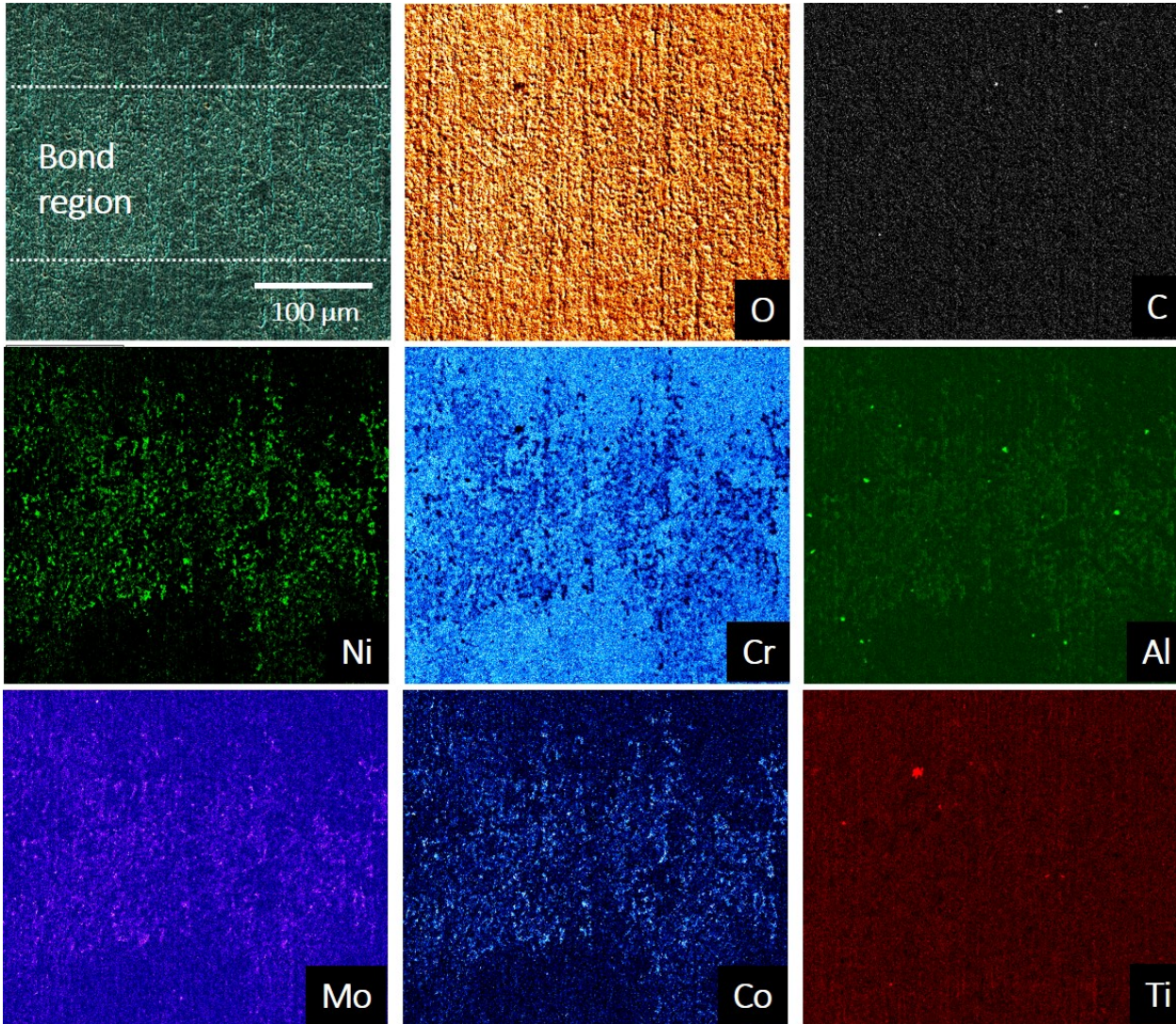
SEM on the surface of oxidized samples – H230-DB-Ni



Slight Ni enrichment and Cr depletion were detected using x-ray elemental mapping on the bond regions of the H230-DB-Ni. The other elements did not show a detectable variation.

Ni plating was 2-4 μm (4-8 μm total for each bond), so bond area reflects diffusion zone

SEM on the surface of oxidized samples – H282-DB-Ni

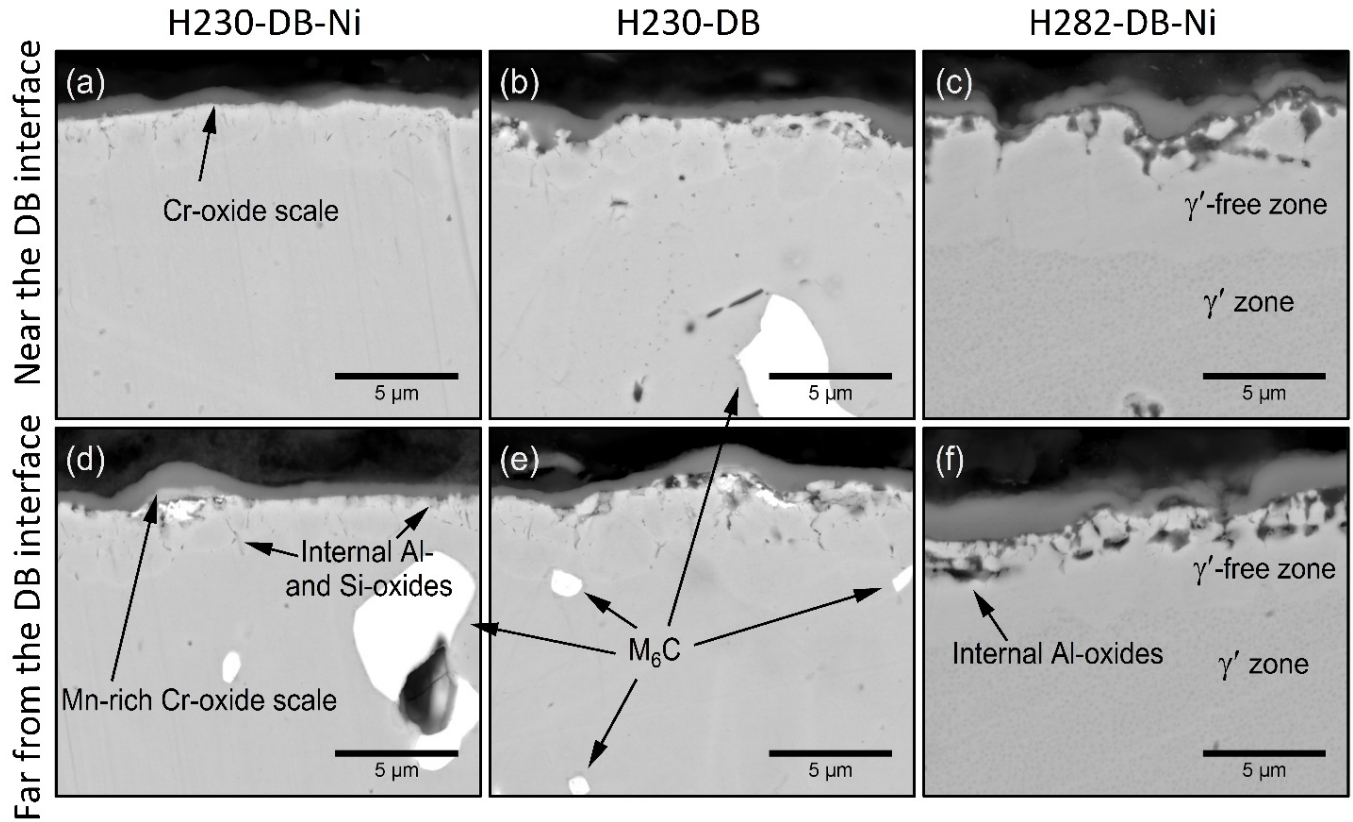


Elemental X-ray maps
acquired on one of the
bond regions of the
H282-DB-Ni coupon
after the 500 h CO₂
exposure at 700°C.

Enrichment of Ni, Al,
Mo, Co in the bond
region

Lower Cr in bond region

SEM on the cross-sections of oxidized samples



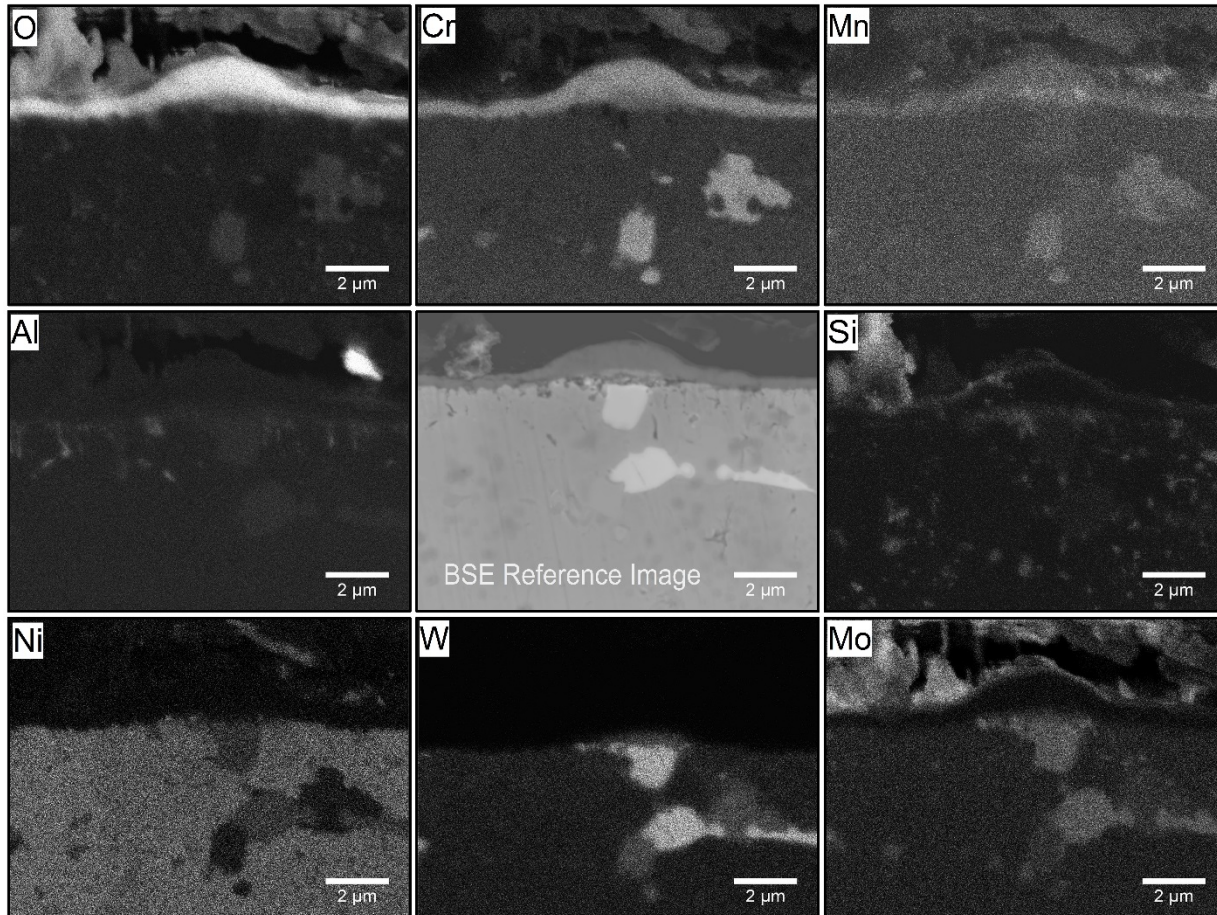
No significant difference between bond regions and away from bond regions

More internal oxidation in H282, resulting from higher Al and Ti levels

γ' loss in H282 below the internal oxidation layer

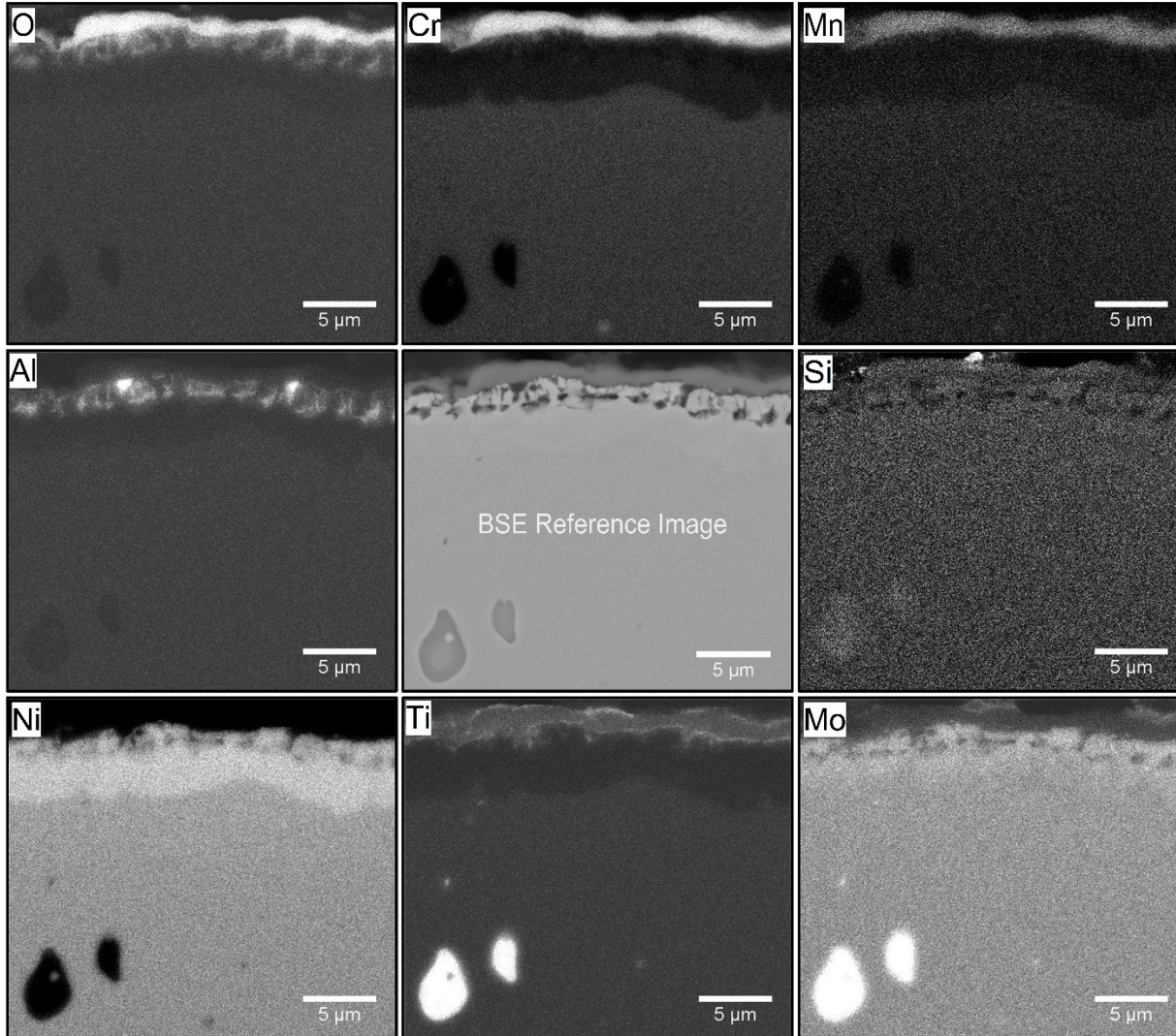
Back-Scattered Electron Images

SEM on the cross-sections of oxidized samples – H230-DB-Ni



X-ray maps of select elements for H230-DB-Ni far from the DB interface. W and Si were acquired in WDS mode and all other elements were collected in EDS mode.

SEM on the cross-sections of oxidized samples – H282-DB-Ni



X-ray (EDS) maps of select elements for H282-DB-Ni far from the DB interface

- **As determined after a 500 h exposure to CO₂ at 700°C, diffusion bonding was not detrimental to the oxidation resistance of the H230. The diffusion bond regions of H230 did not exhibit an accelerated oxidation.**
- **Diffusion bonding of H282 resulted in increased mass gains during oxidation. However, a chromia scale was still formed, and overall oxidation rates were still low.**

Materials Degradation in Supercritical CO₂ Power Cycles

Materials Science and Technology (MS&T) Conference

October 23-27, 2016

Salt Lake City, Utah

Abstracts are due on March 31, 2016

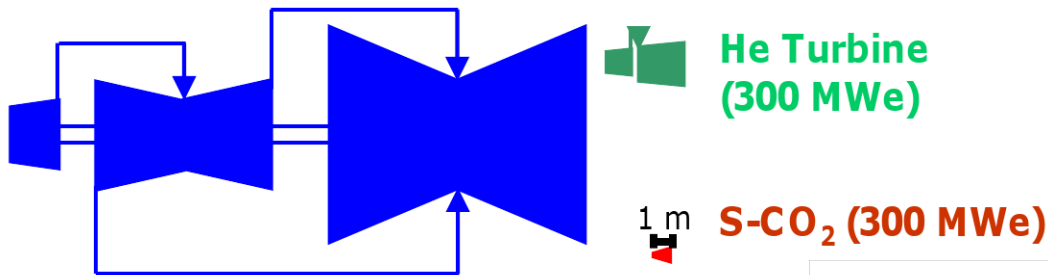
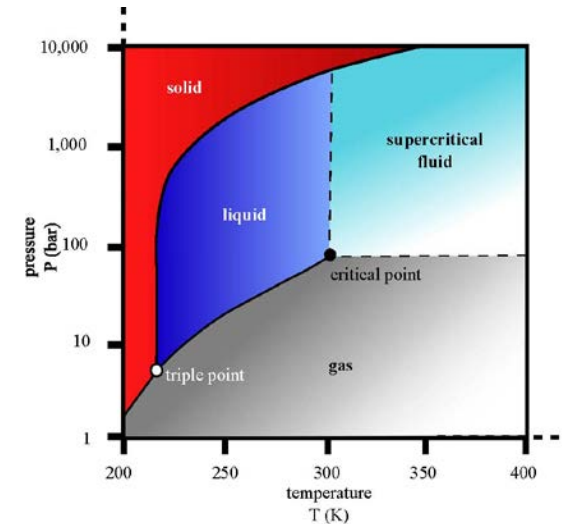
and can be submitted on ProgramMaster :

<http://www.programmaster.org/PM/PM.nsf/Home?OpenForm&ParentUNID=F9FD0D2AAFA2D29285257D86004BE7A3>

Supercritical CO₂ Power Cycles

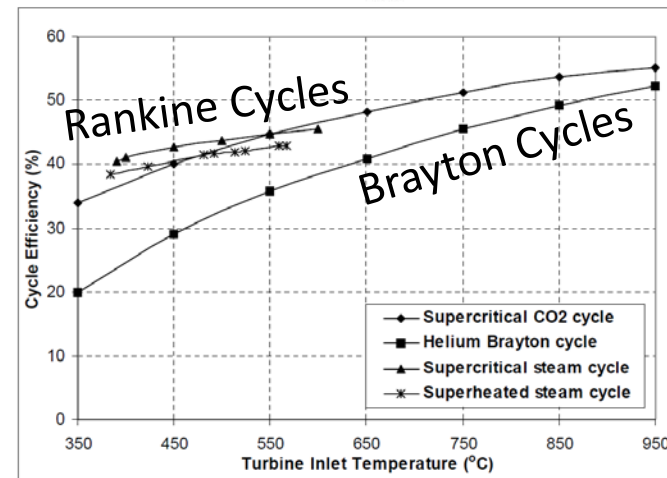


Properties of sCO ₂ Cycles	Impact
No phase change (Brayton Cycle)	Higher efficiency
Recompression near liquid densities	Higher efficiency
High heat recuperation	Higher efficiency Large HX footprint
Compact turbo machinery	Lower capital cost
Simple configurations	Lower capital cost
Dry/reduced water cooling	Lower environmental impact
Storage ready CO ₂ in direct cycles	Lower environmental impact



Steam Turbine (250 MWe)

S. A. Wright, "OVERVIEW OF SUPERCRITICAL CO₂ POWER CYCLE DEVELOPMENT AT SANDIA NATIONAL LABORATORIES," in *2011 University Turbine Systems Research Workshop*, Columbus, Ohio, 2011.



M. J. Driscoll, "Optimized, Competitive Supercritical-CO₂ Cycle GFR for Gen IV Service," MIT-GFR-045, 2008.